

# A small interfering RNA screen for modulators of tumor cell motility identifies MAP4K4 as a promigratory kinase

Cynthia S. Collins\*<sup>†</sup>, Jiyong Hong\*<sup>†§</sup>, Lisa Sapinoso\*, Yingyao Zhou\*, Zheng Liu\*, Kenneth Micklash\*, Peter G. Schultz\*<sup>‡</sup>, and Garret M. Hampton\*<sup>†¶</sup>

\*Genomics Institute of the Novartis Research Foundation, 10675 John Jay Hopkins Drive, San Diego, CA 92121; and <sup>‡</sup>Department of Chemistry and The Skaggs Institute for Chemical Biology, The Scripps Research Institute, 10550 North Torrey Pines Road, SR202, La Jolla, CA 92037

Communicated by Webster K. Cavenee, University of California at San Diego, La Jolla, CA, January 3, 2006 (received for review December 5, 2005)

Cell motility is a complex biological process, involved in development, inflammation, homeostasis, and pathological processes such as the invasion and metastatic spread of cancer. Here, we describe a genomic screen designed to identify inhibitors of cell migration. A library of 10,996 small interfering RNAs (targeting 5,234 human genes) was screened for their ability to block the migration of a highly motile ovarian carcinoma cell line, SKOV-3, by using a 384-well wound-healing assay coupled with automated microscopy and wound quantification. Two or more small interfering RNAs against four genes, *CDK7*, *DYRK1B*, *MAP4K4* (*NIK/HGK*) (*MAP4K4*, mitogen-activated protein 4 kinase 4), and *SCCA-1* (*Serp1B3*), potently blocked the migration of SKOV-3 cells, concordant with reduced transcript levels. Further studies of the promigratory role of *MAP4K4* showed that the knockdown of this transcript inhibited the migration of multiple carcinoma cell lines, indicating a broad role in cell motility and potently suppressed the invasion of SKOV-3 cells *in vitro*. The effect of *MAP4K4* on cellular migration was found to be mediated through c-Jun N-terminal kinase, independent of AP1 activation and downstream transcription. Accordingly, small molecule inhibition of c-Jun N-terminal kinase suppressed SKOV-3 cell migration, underscoring the potential therapeutic utility of mitogen-activated protein kinase pathway inhibition in cancer progression.

automated | RNA interference

Cell migration is triggered by a diverse array of cell autonomous and environmental cues, culminating in cycles of microfilament and microtubule reorganization, polarization of the secretory pathway, membrane extension, adhesion to the substratum, and retraction (1, 2). Transduction of promigratory stimuli through one of several key pathways [e.g., the mitogen-activated protein kinase (MAPK) pathway] engages the highly conserved Rho GTPases, Rac1, RhoA, and Cdc42, which integrate these signals with dynamic reorganization of the cytoskeleton (2). Many of the components of these signaling pathways that promote cell migration are commonly activated in tumor cells through mutation or overexpression of promigratory kinases (e.g., Met, Src, and fibroblast and epidermal growth factor receptors), mutation of Ras GTPases, or loss of tumor suppressors, such as the PTEN phosphatase (reviewed in ref 3). Activation of these pathways, and the consequent increase in cell motility, is highly correlated with tissue invasion and distant metastasis (3). Thus, dissecting tumor cell motility is likely to provide important insights into metastatic development.

Cell migration can be monitored by a number of assays *in vitro* and *in vivo*, ranging from microscopic observation of movement on a 2D substrate to intravital imaging in rodents (3). One of simplest, termed the wound-healing assay (4), is widely used to monitor the migratory potential of cells, requiring only the introduction of a scratch across the surface of a confluent cell monolayer with a pipette tip, or other blunt instrument, followed by movement of cells across the denuded surface to “heal” the

wound. Here, we automated the wound-healing assay to monitor tumor cell migration in 384-well plates by using a custom-built “scratch” device, coupled with automated image capture and quantification of cellular migration. This automated phenotypic screen was used to interrogate the migratory suppression of  $\approx 11,000$  small interfering RNAs (siRNAs) in the highly migratory ovarian carcinoma cell line SKOV-3, resulting in the identification and validation of four previously undescribed promigratory genes, including the mitogen-activated kinase, *MAP4K4* (also called nck-interacting kinase or hepatocyte progenitor kinase-like/germinal center kinase-like kinase), whose role in cancer cell motility was further characterized.

## Results

**Development of an Automated Cell Migration Assay.** Measurement of cell migration by the wound-healing assay (4) was automated by using a custom-built, 384-well scratch device, coupled to automated image capture and quantification of wound closure (see Fig. 7 and *Supporting Materials and Methods*, which are published as supporting information on the PNAS web site). The assay system utilizes a precision-drilled aluminum block into which 384 pipette tips are inserted and fastened. The block is lowered on a static arm into the wells of a 384-well plate containing confluent cell monolayers and shunted  $\approx 3$  mm by hydraulic pressure. After the wounds are allowed to close, the cells are fixed and stained with the nuclear stain, DAPI, to enable rapid image capture by automated microscopy.

To validate the assay, the temporal migration of a highly motile ovarian carcinoma-derived cell line, SKOV-3, was monitored in the presence of siRNAs, small molecules and appropriate controls. The efficacy of siRNA-mediated migratory inhibition was assessed by using siRNAs homologous to Rac1, one of three Rho GTPases (RhoA, Rac1, and Cdc42) that integrates promigratory signals with dynamic reorganization of the actin cytoskeleton (ref. 2; Fig. 1A). In addition, we tested known small molecule inhibitors of c-Src (SKI-606, ref. 6; and a 2-phenyl-aminoimidazo-[4,5-h]-isoquinolin-9-one, termed compound 43, ref. 7), the activated form of which plays a central role in the motility and invasion of cancer cells, including ovarian (refs. 7 and 8; Fig. 1A). Using a pixel density-based quantitative measure of cell migration (see *Supporting Materials and Meth-*

Conflict of interest statement: No conflicts declared.

Freely available online through the PNAS open access option.

Abbreviations: JNK, c-Jun N-terminal kinase; MAPK, mitogen-activated protein kinase; siRNA, small interfering RNA.

<sup>†</sup>C.S.C. and J.H. contributed equally to this work.

<sup>§</sup>Present address: Department of Chemistry, Duke University, 101 Gross Chem, Box 90347, Durham, NC 27708.

<sup>¶</sup>To whom correspondence should be sent at the present address: Celgene Signal Research, 4550 Towne Centre Drive, San Diego, CA 92121. E-mail: ghampton@celgene.com.

© 2006 by The National Academy of Sciences of the USA

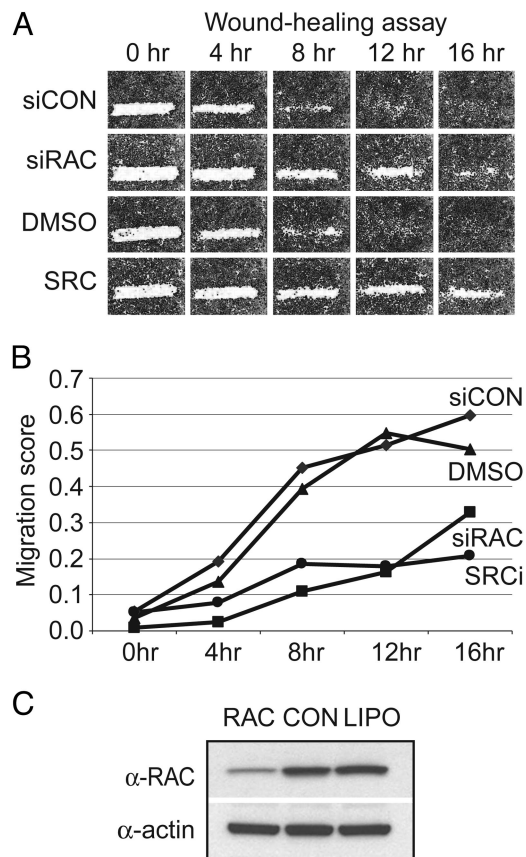


**Fig. 1.** Validation of the automated cell motility assay. (A) The temporal (0, 4, 8, 12, and 16 h) migration of SKOV-3 cells in the presence and absence of controls is shown. siCON, FITC-conjugated control siRNA; siRAC, a sequence-specific siRNA targeting RAC; DMSO, dimethyl sulfoxide; SRC, c-Src family kinase inhibitor, compound 43 (5). (B) Quantification of SKOV-3 migration. The degree of scratch closure ("migration score") was determined by an automated algorithm and plotted as a function of time. Low migration scores reflect migratory inhibition. (C) Western blot demonstrating knockdown of the RAC protein by the RAC-specific siRNA used in A, compared to a control siRNA (CON) and mock transfected cells (LIPO). The same blot reprobed with an anti-actin antibody to demonstrate equal loading is shown below.

ods), the addition of the Rac1 siRNA pool or the Src inhibitors retarded SKOV-3 cell migration by 60–70%, respectively, at 12 h after scratching (relative to control wells at the same time points; Fig. 1B). Although migratory inhibition is evident at 8 and 16 h, 12 h represented the largest difference between controls and test siRNAs at a time point where control cells closed the wound. In parallel, we measured cell viability in identically treated 384-well plates by using an ATP-based luminescent assay to monitor potential toxic effects of siRNA transfection and small molecule inhibition on SKOV-3 cells. All screen controls shown in Fig. 1 did not have an appreciable effect on cell viability (luminescent signal was >90% of untreated well signal).

The reproducibility of the assay was tested by using a diverse subset of 384 preplated siRNAs targeting 192 genes (two siRNAs per gene plated in duplicate). For these experiments, SKOV-3 cells were reverse transfected on each of three replicate plates, grown to confluency, wounded, and incubated for a further 12 h. After image capture, wells from each of the three replicate plates were scored by the quantitative algorithm (see *Supporting Materials and Methods*) and the score from each individual well in each of the three replicate runs was compared to the mean well score by using the Pearson correlation coefficient. In each case,  $r^2$  was >0.87, demonstrating a high degree of well-to-well

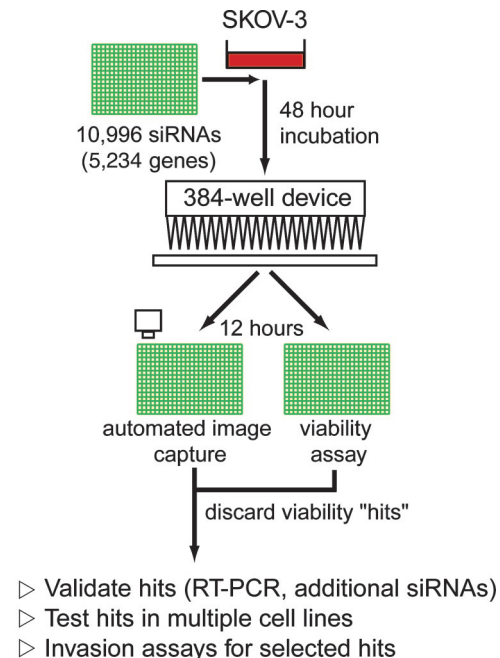


**Fig. 2.** Schematic of the SKOV-3 siRNA screen and followup.

consistency (Fig. 8, which is published as supporting information on the PNAS web site).

**A Large-Scale siRNA Screen for Inhibitors of SKOV-3 Cell Motility.** We used a preplated library of 10,996 siRNAs, targeting 5,234 genes (described in *Supporting Materials and Methods*) to identify inhibitors of cellular motility in SKOV-3 cells (Fig. 2). Cells were reverse transfected as described above and incubated for 48 h before wounding. The screen was performed in duplicate ( $\approx 22,000$  wells) and quantitatively scored. Measurement of cell viability was performed in a set of duplicate siRNA library plates, and the luminescence of each well was compared to the normalized mean well intensity of each 384-well plate. To eliminate siRNAs that induced cell growth arrest or cell death and would not migrate as a consequence, we adopted a viability cutoff score of 0.9 (10% deviation from the plate mean), below which siRNAs were disregarded.

The top  $\approx 5\%$  of wells in which SKOV-3 cells migrated the least ( $n = 532$ ), were chosen for further analysis (Table 1, which is published as supporting information on the PNAS web site), based on a statistical review of the screen (see *Supporting Materials and Methods*). Because of the significant potential for off-target effects when considering the phenotypic effects of single siRNAs, we focused only on those transcripts targeted by at least two independent siRNA sequences ( $n = 22$ ), with the assumption that a similar phenotypic effect observed with two siRNAs would be less likely to occur by chance (Table 2, which is published as supporting information on the PNAS web site). To test this assumption, we resynthesized the siRNAs from the library sequences and monitored transcript knockdown by semi-quantitative RT-PCR in parallel with migratory inhibition. Of the 46 siRNAs targeting 22 genes (20 genes targeted by 2 siRNAs and 2 genes targeted by 3 siRNAs), 36 (78%; 17 unique genes) yielded migratory phenotypes similar to those observed in the primary screen. In contrast to the high degree of concordance at a phenotypic level, independent siRNAs against only 4 of the 22 genes; *MAP4K4*, *DYRK1B*, *CDK7*, and *SerpinB3*, exhibited similar reductions in transcript levels, consistent with phenotypic inhibition (Fig. 3A).



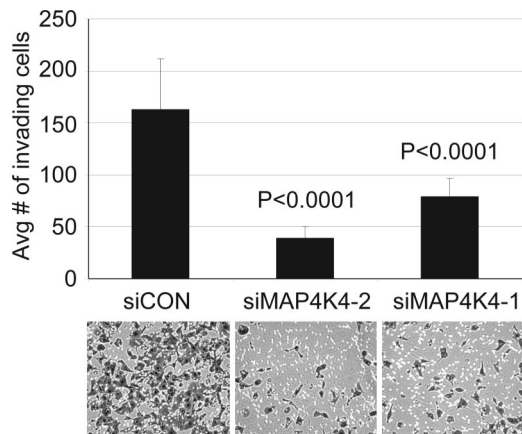


**Fig. 5.** Down-regulation of MAP4K4 decreases SKOV-3 cell invasion *in vitro*. Cells transiently transfected with siRNAs were subjected to Boyden chamber assays of cell invasion through matrigel. The data were collected from five individual consecutive fields of view ( $\times 10$  objective) of each of four replicate invasion chambers. Representative photomicrographs are shown beneath the graph.

the cells. This effect on SKOV-3 migration is consistent with the effect of SP600125 on JNK-dependent cellular migration in NBT-II bladder tumor cells, MDA-MB-231 cells, fish keratinocytes ( $50 \mu\text{M}$ ) (13), and fibroblasts ( $20 \mu\text{M}$ ) (14). These results, together with the observation that siRNAs targeting Rac1 inhibit SKOV-3 migration (Fig. 1), tentatively suggest a constitutively active Rac1-MEKK1-JNK pathway in SKOV-3 cells. However, additional work is required to substantiate whether the major effect is mediated via JNK and whether constitutively activated JNK can rescue the migration of cells with diminished MAP4K4.

We next asked whether the effect of JNK on SKOV-3 migration was mediated through activation of AP1 transcription. To first

address this question, the expression profile of cells transiently transfected with two MAP4K4 siRNAs (si.1 and si.2) was assessed by oligonucleotide microarray hybridization on a 22,500-member array. We did not observe modulation of any known AP1 target genes; indeed, the only significantly altered probe sets when compared to control cells were those homologous to the MAP4K4 transcript, strongly indicating a lack of AP1-mediated transcription. Basal c-Jun protein and phosphoprotein levels were essentially undetectable by Western blot in SKOV-3 cells (data not shown), further confirming the lack of AP1 activation.

MAP4K4 has also been reported to activate a number of other proteins, including kinases within the JAK/STAT pathway. Because JAK/STAT signaling is highly active in high grade ovarian carcinomas and has been shown to be important for SKOV-3 cell motility by RNA interference-mediated knock-down (15), we examined the phosphorylation of STAT-3 in the presence or absence of MAP4K4 siRNAs. No significant changes were observed (Fig. 7), further supporting a major role for JNK in mediating SKOV-3 cell motility.

## Discussion

Epithelial tumor progression depends on the sequential acquisition of multiple cellular traits, including the dissolution of cell-cell contacts and increased motility, enabling the invasion of adjacent tissues and, ultimately, the colonization of distant body sites. To address the underlying molecular mechanisms that promote cancer cell motility, we developed an automated 384-well wound-healing assay, coupled with automated microscopy and quantification.

We queried a custom library of 10,996 synthetic siRNAs targeting 5,234 transcripts to identify genes involved in the migration of SKOV-3 cells, a highly motile cell line derived from the ascites of a patient with metastatic ovarian adenocarcinoma. Although we identified 532 siRNAs with highly significant effects on migration (i.e., the highest ranked 5%; see *Supporting Materials and Methods*), which included many genes known to play a role in cell motility, we chose to examine the 22 genes targeted by at least two siRNAs, because of the significant potential for off-target phenotypic effects elicited by a single siRNA. Evaluation of resynthesized siRNAs targeting these 22 genes showed a relatively high degree of phenotypic consistency (74%), but a much lower consistency in terms of correlated transcriptional knockdown and migratory suppression of both siRNAs. Four genes, *CDK7*, *MAP4K4*, *DYRK1B*, and *SerpinB3*, were validated by these criteria. Given the apparently high off-target rate, we anticipate that future screens should encompass additional siRNAs against each target or secondary screens designed to interrogate the subgroup of identified hits (532 in this case) with additional, independent siRNAs.

We chose to further examine the role of MAP4K4 in cancer cell motility primarily because the protein is involved developmental cell migration (7) and is reported to augment cellular motility and invasion of rat intestinal epithelial cells in the presence of hepatocyte growth factor (8). Cumulatively, our data show that MAP4K4 is involved in the motility of multiple cancer cell lines, signaling upstream of JNK, and that inhibition of MAP4K4 results in suppression of invasion *in vitro*. Activation of JNK by MAP4K4 has been shown previously; however, it is reported to be indirect, acting through TAK1, MKK4, and MKK7 (11). However, we have been unable to detect appreciable basal levels of phospho-MKK4 or phospho-MKK7 (data not shown), suggesting that MAP4K4 may activate JNK through other kinases, at least in this cell type. Downstream of JNK, we have shown that AP1-dependent transcription is not involved in SKOV-3 cell migration; however, the substrates through which MAP4K4-JNK mediates its effects are not yet defined. Multiple direct targets of JNK phosphorylation have been described (reviewed in ref. 9), including the microtubule-associated pro-

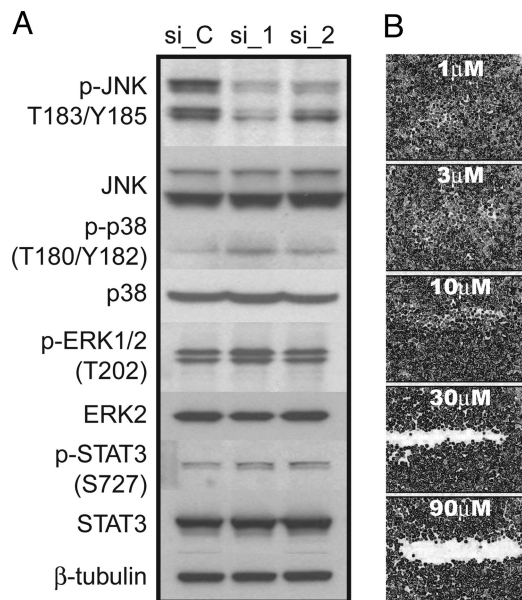


**Fig. 6.** Decrease in JNK phosphorylation after siRNA-mediated knockdown of *MAP4K4*. (A) Western blots of SKOV-3 total protein lysates collected 48 h after transfection with control (si\_C) or MAP4K4-specific siRNAs (si.1 and si.2). Blots were probed with phospho-specific antibodies (p) and antibodies recognizing total JNK, p38, ERK, and STAT-3. (B) Scratch migration assay of SKOV-3 cells exposed to increasing concentrations of the JNK inhibitor, SP600125.



We thank Drs. Quinn Deveraux, Christopher Stroh, and Venkat Reddy for critically reading the manuscript and Drs. Pedro Aza-Blanc, Serge

Batalov, and Sumit Chanda, Mr. Abel Gutierrez, and Mr. Paul deJesus for siRNA design, library construction, assay development, and advice.

1. Lauffenburger, D. A. & Horwitz, A. F. (1996) *Cell* **84**, 359–369.
2. Ridley, A. J., Schwartz, M. A., Burridge, K., Firtel, R. A., Ginsberg, M. H., Borisy, G., Parsons, J. T. & Horwitz, A. R. (2003) *Science* **302**, 1704–1709.
3. Sahai, E. (2005) *Curr. Opin. Genet. Dev.* **15**, 87–96.
4. Todaro, G. J., Lazar, G. K. & Green, H. (1965) *J. Cell. Physiol.* **66**, 325–333.
5. Goldberg, D. R., Butz, T., Cardozo, M. G., Eckner, R. J., Hammach, A., Huang, J., Jakes, S., Kapadia, S., Kashem, M., Lukas, S., *et al.* (2003) *J. Med. Chem.* **46**, 1337–1349.
6. Golas, J. M., Lucas, J., Etienne, C., Golas, J., Discafani, C., Sridharan, L., Boghaert, E., Arndt, K., Ye, F., Boschelli, D. H., *et al.* (2005) *Cancer Res.* **65**, 5358–5364.
7. Wiener, J. R., Windham, T. C., Estrella, V. C., Parikh, N. U., Thall, P. F., Deavers, M. T., Bast, R. C., Mills, G. B. & Gallick, G. E. (2003) *Gynecol. Oncol.* **88**, 73–79.
8. Xue, Y., Wang, X., Li, Z., Gotoh, N., Chapman, D. & Skolnik, E. Y. (2001) *Development (Cambridge, U.K.)* **128**, 1559–1572.
9. Wright, J. H., Wang, X., Manning, G., LaMere, B. J., Le, P., Zhu, S., Khatri, D., Flanagan, P. M., Buckley, S. D., Whyte, D. B., *et al.* (2003) *Mol. Cell. Biol.* **23**, 2068–2082.
10. Huang, C., Jacobson, K. & Schaller, M. D. (2004) *J. Cell Sci.* **117**, 4619–4628.
11. Favata, M. F., Horiuchi, K. Y., Manos, E. J., Daulerio, A. J., Stradley, D. A., Feeser, W. S., Van Dyk, D. E., Pitts, W. J., Earl, R. A., Hobbs, F., *et al.* (1998) *J. Biol. Chem.* **273**, 18623–18632.
12. Yao, Z., Zhou, G., Wang, X. S., Brown, A., Diener, K., Gan, H. & Tan, T. H. (1999) *J. Biol. Chem.* **274**, 2118–2125.
13. Huang, C., Rajfur, Z., Borchers, C., Schaller, M. D. & Jacobson, K. (2003) *Nature* **424**, 219–223.
14. Javelaud, D., Laboureau, J., Gabison, E., Verrecchia, F. & Mauviel, A. (2003) *J. Biol. Chem.* **278**, 24624–24628.
15. Burke, W. M., Jin, X., Lin, H. J., Huang, M., Liu, R., Reynolds, R. K. & Lin, J. (2001) *Oncogene* **20**, 7925–7934.
16. Poinat, P., De Arcangelis, A., Sookhareea, S., Zhu, X., Hedgecock, E. M., Labouesse, M. & Georges-Labouesse, E. (2002) *Curr. Biol.* **12**, 622–631.
17. Aza-Blanc, P., Cooper, C. L., Wagner, K., Batalov, S., Deveraux, Q. L. & Cooke, M. P. (2003) *Mol. Cell* **12**, 627–637.